

# An Approach to Dendritic Oligosilanes: Controlling the Conformation through Ring Formation

C. Krempner\* and H. Reinke

Institut für Chemie der Universität Rostock, A.-Einstein-Strasse 3a, D-18059 Rostock, Germany

Received October 21, 2006

The synthesis, solid-state structure, and UV spectroscopic properties of the first-generation single-core oligosilane dendrimer  $\text{MeSi}[\text{SiMe}_2\text{Si}(\text{SiMe}_3)_2\text{Me}]_2[\text{SiMe}_2\text{Si}(\text{SiMe}_3)_3]$  (**5**) and the tethered analogue  $(\text{CH}_2)_4[\text{Si}(\text{SiMe}_3)_2\text{SiMe}_2]_2\text{Si}[\text{SiMe}_2\text{Si}(\text{SiMe}_3)_3]\text{Me}$  (**4**) are reported. UV spectroscopic measurements in solution and in the solid state (diffuse reflectance) show the absorption maximum of tetramethylene-tethered **4** to be shifted to wavelengths longer than those of **5**, the dendrimers  $\text{MeSi}[\text{SiMe}_2\text{Si}(\text{SiMe}_3)_3]_3$  (**6**) and  $\text{MeSi}[\text{SiMe}_2\text{Si}(\text{SiMe}_3)_2\text{Me}]_3$  (**7**), and even that of the linear heptasilane  $\text{Si}_7\text{Me}_{16}$ . This can be explained by the results of the X-ray analysis of **4** and **5**, which reveal for **4** the presence of an A–D–A–D conformer, which is optimal for  $\sigma$ -conjugation, whereas in **5** only D–D–O–D conformers have been found.

## Introduction

One of the most characteristic features of oligo- and polysilanes is the extensive delocalization of  $\sigma$ -electrons ( $\sigma$ -conjugation) along the silicon main chain, resulting in unique optoelectronic properties such as intense emissions and absorptions in the near-UV region.<sup>1</sup> Their electronic absorptions were found to be sensitive to the conformation of the silicon backbone, as reflected in the thermochromism of some linear derivatives.<sup>2</sup> In fact, recent studies of linear oligosilanes with discrete conformations have shown  $\sigma$ -conjugation to be effectively extended by an anti conformation (Si–Si–Si–Si dihedral angle  $\omega = 180^\circ$ ), while conformations with small dihedral angles such as syn, cisoid, or even gauche ( $\omega = 0\text{--}60^\circ$ ) do not contribute significantly.<sup>3</sup>

However, describing the relationship between conformation and photophysical properties of oligosilane dendrimers,<sup>4</sup> a relatively new class of highly branched organosilicon compounds that combine similar photophysical properties with good solubility and high thermal and chemical resistance, seems to be rather challenging. Difficulties in interpreting their UV spectra, which usually show very broad and intense absorption maxima, mainly arise from the redundancy of Si–Si chains realized in these molecules. This results in a statistical distribution of highly flexible conformers, each contributing differently to the extent of  $\sigma$ -conjugation along the Si–Si backbone. Controlling the silicon backbone conformation in these branched architectures would be highly desirable, because it would allow

the assignment of distinct absorption bands as being associated with the existence of different conformers, as we have shown very recently for structurally similar hydroxy-functionalized oligosilane dendrimers.<sup>5</sup> Several approaches have been introduced to control the silicon backbone conformation of linear oligosilanes such as inclusion into cyclodextrins,<sup>6</sup> conformational locking by hydrogen bond interactions,<sup>5</sup> and incorporation of pentacoordinate silicon atoms<sup>7</sup> or of cyclic and bicyclic structures.<sup>3</sup> In particular, the last approach, introduced by Michl and by Tamao, proved to be the most successful, as demonstrated for various all-anti conformers of different chain lengths that could be obtained by incorporating tethering groups  $(\text{CH}_2)_n$  ( $n = 1\text{--}4$ ). Herein, we report the synthesis, structure, and photophysical properties of a new first-generation single-core oligosilane dendrimer and its tetramethylene-tethered analogue.

## Results and Discussion

The synthetic route to the tethered oligosilane **4** is outlined in Scheme 1. The reaction of  $\text{KSi}(\text{SiMe}_3)_3$  with  $\text{MeSi}(\text{SiMe}_2\text{Cl})_3$  in a 1:1 ratio furnished the dichloro-functionalized oligosilane **1** in a 69% yield. In analogy to the procedure described by Mechtler and Marschner,<sup>8</sup> the bis(hypersilyl)butane **2** was converted to the corresponding dipotassium disilanide **3** by treatment with 2 equiv of  $\text{KOBu}^t$  in THF at  $60\text{--}65^\circ\text{C}$ . Finally, compound **3** was reacted with **1** to give **4** in moderate yield (28%). The synthesis of dendrimer **5** was affected by adding 2 equiv of  $\text{KSi}(\text{SiMe}_3)_2\text{Me}$  to a solution of **1** in pentane at  $-78$

\* To whom correspondence should be addressed. Fax: +49 (0)381 498 6382. Tel: +49 (0)381 498 6385. E-mail: clemens.krempner@uni-rostock.de.

(1) (a) Miller, R. D.; Michl, J. *Chem. Rev.* **1989**, *89*, 1359. (b) West, R. In *The Chemistry of Organic Silicon Compounds*; Patai, S., Rappoport, Z., Eds.; Wiley: Chichester, U.K., 1989; p 1207.

(2) Bukalov, S. S.; Leites, L. A.; West, R. *Macromolecules* **2001**, *34*, 6003 and references therein.

(3) (a) Mazieres, S.; Raymond, M. K.; Raabe, G.; Prodi, A.; Michl, J. *J. Am. Chem. Soc.* **1997**, *119*, 6682. (b) Tamao, K.; Tsuji, H.; Terada, M.; Asahara, M.; Yamaguchi, S.; Toshimitsu, A. *Angew. Chem.* **2000**, *112*, 3425; *Angew. Chem., Int. Ed.* **2000**, *39*, 3287. (c) Tsuji, H.; Terada, M.; Toshimitsu, A.; Tamao, K. *J. Am. Chem. Soc.* **2003**, *125*, 7486. (d) Fukazawa, A.; Tsuji, H.; Tamao, K. *J. Am. Chem. Soc.* **2006**, *128*, 6800.

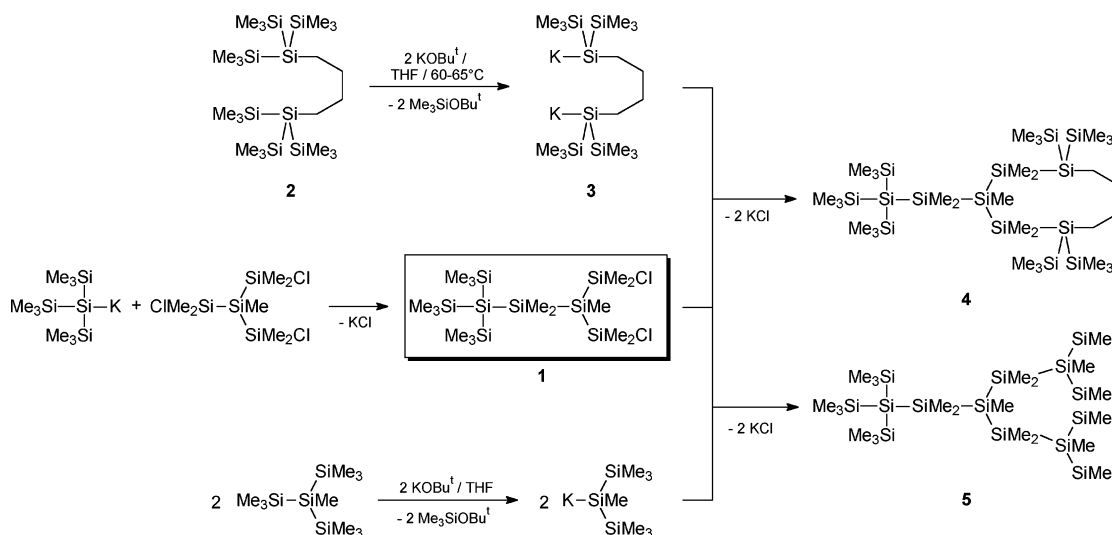
(4) For a microreview see: Lambert, J. B.; Pflug, J. L.; Wu, H.; Liu, X. *J. Organomet. Chem.* **2003**, *685*, 113.

(5) Jäger-Fiedler, U.; Wulff, A.; Köckerling, M.; Ludwig, R.; Krempner, C. *Angew. Chem., Int. Ed.* **2006**, *45*, 6755.

(6) (a) Okumura, H.; Kawaguchi, Y.; Harada, A. *Macromol. Rapid Commun.* **2002**, *23*, 781. (b) Okumura, H.; Kawaguchi, Y.; Harada, A. *Macromolecules* **2003**, *36*, 6422. (c) Sakamoto, T.; Naruoka, T.; Kira, M. *Chem. Lett.* **2003**, *32*, 380. (d) Sanji, T.; Yoshiwara, H.; Sakurai, H.; Tanaka, M. *Chem. Commun.* **2003**, 1506. (e) Sanji, T.; Kato, N.; Kato, M.; Tanaka, M. *Angew. Chem., Int. Ed.* **2005**, *44*, 7301. (f) Sanji, T.; Kato, M.; Tanaka, M. *Macromolecules* **2005**, *38*, 4034. (g) Sanji, T.; Kato, M.; Tanaka, M. *Macromolecules* **2006**.

(7) (a) El Sayed, I.; Hatanaka, Y.; Muguruma, C.; Shimada, S.; Tanaka, M.; Koga, N.; Mikami, M. *J. Am. Chem. Soc.* **1999**, *121*, 5095. (b) El Sayed, I.; Hatanaka, Y.; Onozawa, S.-Y.; Tanaka, M.; Koga, N.; Mikami, M. *J. Am. Chem. Soc.* **2001**, *123*, 3597.

(8) Mechtler, C.; Marschner, C. *Tetrahedron Lett.* **1999**, *40*, 7777.

Scheme 1. Synthesis of the Dendrimers **4** and **5**

°C. Both compounds are thermally stable, colorless solids. The expected bond lengths of **4** and **5** were confirmed by means of multinuclear NMR spectroscopy. The  $^{29}\text{Si}$  NMR spectra are particularly useful, because they permit assigning silicon atoms to the number of methyl groups (see Experimental Section).

In addition, the solid-state structures of **4** and **5** were determined unambiguously by X-ray crystallography; suitable single crystals were grown from ethyl acetate solutions at room temperature. The molecular structures along with selected bond distances and angles are shown in Figures 1 and 2. The tethered

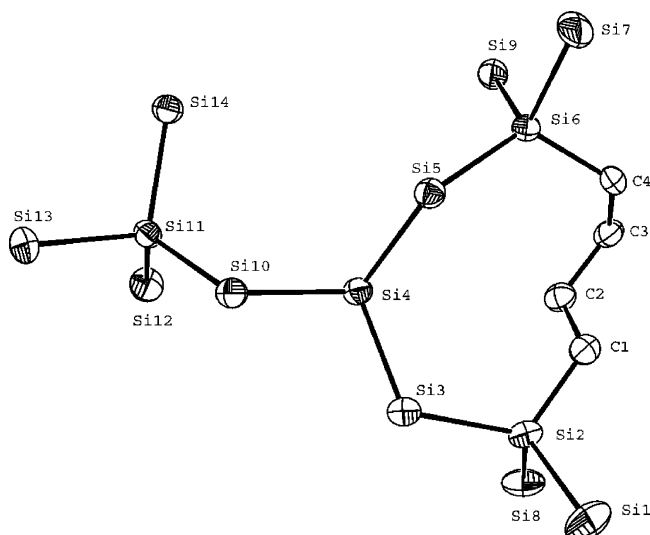


**Figure 1.** Molecular structure of **4** in the crystal state (ORTEP, 30% probability level, all methyl groups omitted for clarity). Selected bond lengths (Å), bond angles (deg), and torsion angles (deg): Si3–Si4 = 2.371(2), Si4–Si5 = 2.411(2), Si4–Si10 = 2.392(2), Si5–Si6 = 2.390(2), Si6–Si7 = 2.381(2), Si10–Si11 = 2.377(2), Si11–Si13 = 2.371(2); Si2–Si3–Si4 = 116.35(7), Si6–Si5–Si4 = 125.71(7), Si9–Si6–Si5 = 116.97(7), Si11–Si10–Si4 = 116.10(7), Si14–Si11–Si10 = 114.06(6), Si12–Si11–Si10 = 114.23(6); Si8–Si2–Si3–Si4 = 94.04(8), Si2–Si3–Si4–Si5 = 60.79(9), Si3–Si4–Si5–Si6 = 96.80(9), Si10–Si4–Si5–Si6 = 148.41(7), Si4–Si5–Si6–Si9 = 57.33(10), Si4–Si5–Si6–Si7 = 177.77(7), Si5–Si4–Si10–Si11 = 99.34(8), Si4–Si10–Si11–Si14 = 63.58(9), Si4–Si10–Si11–Si12 = 60.73(9), Si1–Si2–Si3–Si4 = 146.34(7), Si2–Si3–Si4–Si10 = 179.73(7), Si3–Si4–Si10–Si11 = 141.27(7), Si4–Si10–Si11–Si13 = 179.37(6).

compound **4** crystallizes in the triclinic space group  $P\bar{1}$  with two unique molecules in the asymmetric unit, each of which has a total of 14 silicon atoms and longest chains of 7 silicon atoms. The molecule contains one  $\text{Si}(\text{SiMe}_3)_3$  unit and two  $\text{Si}(\text{SiMe}_3)_2\text{CH}_2$  units that are nonequivalent in the crystal. The branching points of the latter units are linked by a tetramethylene tether, resulting in the formation of a nine-membered carosilane ring with a boat conformation. Structural parameters indicate considerable steric strain in the molecule. For example, two of three Si–Si bonds emanating from the central core (Si4) in **4** are elongated, Si4–Si5 = 2.411(2) Å and Si4–Si10 = 2.392(2) Å, and also the Si5–Si6 distance within the ring is increased to 2.390(2) Å. The steric strain is reduced by increasing the angles around the central core (Si4). Thus, Si6–Si5–Si4, the angle between the core, the spacer, and the branch silicon of the bulky  $\text{Si}(\text{SiMe}_3)_3$  wing, is 125.71(7)°. Similar structural parameters have been observed for the second molecule of the asymmetric unit.

The structurally analogous dendrimer **5** crystallizes in the monoclinic space group  $C2/c$  and contains a total of 14 silicon atoms and longest chains of 7 silicon atoms. It contains a  $\text{Si}(\text{SiMe}_3)_3$  unit and two  $\text{Si}(\text{SiMe}_3)_2\text{Me}$  wings, the latter being nonequivalent in the crystal. Similar to the case for **4**, the strain in the periphery is reduced by widening the Si–Si–Si angles around the central core (Si4). The largest distortion is observed for the Si6–Si5–Si4 angle (119.30(5)°) and is rather similar to the case for **4**, with the three bonds emanating from the central core atom (Si4) being slightly elongated: Si3–Si4 = 2.384(1) Å, Si5–Si4 = 2.392(1) Å, Si11–Si4 = 2.387(1) Å.

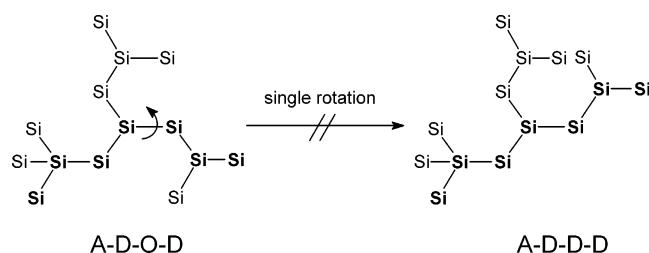
As mentioned above, the elongation of  $\sigma$ -conjugation along the silicon chain in permethylated oligosilanes arises mainly from all-anti conformers, while conformations with small dihedral angles ( $\omega = 0\text{--}60^\circ$ ) do not contribute. To obtain an insight into the relationship between the conformation and electronic properties of dendritic oligosilanes, the conformations of the longest heptasilane chains have been analyzed on the basis of the available X-ray data. The SiSiSiSi dihedral angles of **4** and **5** and, for comparison, those of  $\text{MeSi}[\text{SiMe}_2\text{Si}(\text{SiMe}_3)_3]_3$  (**6**)<sup>9</sup> and  $\text{MeSi}[\text{SiMe}_2\text{Si}(\text{SiMe}_3)_2\text{Me}]_3$  (**7**),<sup>10</sup> along with the calculated average Si–Si distances of the chains, are

(9) (a) Lambert, J. B.; Pflug, J. L.; Stern, C. L. *Angew. Chem., Int. Ed. Engl.* **1995**, *34*, 9. (b) Lambert, J. B.; Pflug, J. L.; Denari, J. M. *Organometallics* **1996**, *15*, 61. (c) Suzuki, H.; Kimata, Y.; Satoh, S.; Kuriyama, A. *Chem. Lett.* **1995**, 293.

**Table 1.** SiSiSiSi Dihedral Angles and Average Si–Si Distances of Selected Heptasilane Chains of 4–7

compd	heptasilane chain	dihedral angle (deg)	symbol	av dist (Å)
4	13–11–10–4–3–2–1	179–141–180–146	A–D–A–D	2.370
	7–6–5–4–10–11–13	178–148–99–179	A–D–O–A	2.387
	1–2–3–4–5–6–7	146–61–97–178	D–G–O–A	2.376
5	7–6–5–4–11–12–13	180–147–82–156	A–D–O–D	2.374
	1–2–3–4–5–6–7	138–162–98–180	D–D–O–A	2.375
6 <sup>9a,b</sup>	13–12–11–4–3–2–1	156–160–82–138	D–D–O–D	2.369
		157–173–64–157	D–A–G–D	2.357
6 <sup>9c</sup>		152–177–62–152	D–A–G–D	2.393
7 <sup>10</sup>		143–161–87–152	D–D–O–D	2.359
		157–152–81–143	D–D–O–D	2.356
		152–156–90–157	D–D–O–D	2.359

summarized in Table 1. Except for **6**, compounds **4**, **5**, and **7** consist of three wings that are crystallographically different. Therefore, three heptasilane chains, namely those with the four largest SiSiSiSi dihedral angles for each possible pathway, are selected. Interestingly, no all-anti conformers have been found in the heptasilane chains in the unconstrained single-core dendrimers **5–7**. The conformational analysis revealed that conformers with exclusively large dihedral angles, such as all-anti (A–A) or all-deviant (D–D) segments, exist only in several pentasilane subunits and that in most of the heptasilane chain anti (A) or deviant (D) segments are interrupted by additional ortho (O) or gauche (G) conformers.<sup>11</sup> In fact, mainly D–D–O–D and D–D–O–A conformers were observed for the unconstrained dendrimers **5–7**. This conformational arrangement can be explained in terms of the bulkiness of the dendrimer wings. They are oriented in the same direction (clockwise or anticlockwise), which reduces their repulsive interactions. From these results it can be stated that the formation of all-anti conformers in unconstrained single-core dendrimers, irrespective of whether they are of first or higher generation,<sup>12</sup> is not preferred, since this would lead to considerable repulsions of the bulky wings (Scheme 2).

**Scheme 2.** Two Conformational Arrangements of **5** (Si=SiMe<sub>n</sub>; n = 1–3)

Returning to tethered **4**, the most remarkable structural feature as compared to **5** arises from a face-to-face orientation of the tethered Si(SiMe<sub>3</sub>)<sub>2</sub>CH<sub>2</sub> units. This leads to a conformational arrangement that is quite different from those in **5** and the other unconstrained single-core dendrimers. In fact, the conformer with the largest dihedral angles of all possible heptasilane pathways is the A–D–A–D conformer, which might be optimal for the delocalization of  $\sigma$ -bonded electrons. The formation of the latter conformer is obviously enforced by the tetramethylene bridging group. It is worth noting that the

(10) Nanjo, M.; Sunaga, T.; Sekiguchi, A.; Horn, E. *Inorg. Chem. Commun.* **1999**, 2, 203.

(11) Following the proposal of Michl and West, the conformations are roughly classified as syn (S,  $\sim 0^\circ$ ), gauche (G,  $\sim 60^\circ$ ), ortho (O,  $\sim 90^\circ$ ), eclipsed (E,  $\sim 120^\circ$ ), deviant (D,  $\sim 150^\circ$ ), and anti (A,  $\sim 180^\circ$ ): Michl, J.; West, R. *Acc. Chem. Res.* **2000**, 33, 821.

(12) (a) Sekiguchi, A.; Nanjo, M.; Kabuto, C.; Sakurai, H. *J. Am. Chem. Soc.* **1995**, 117, 419. (b) Lambert, J. B.; Wu, H. *Organometallics* **1998**, 17, 4904.

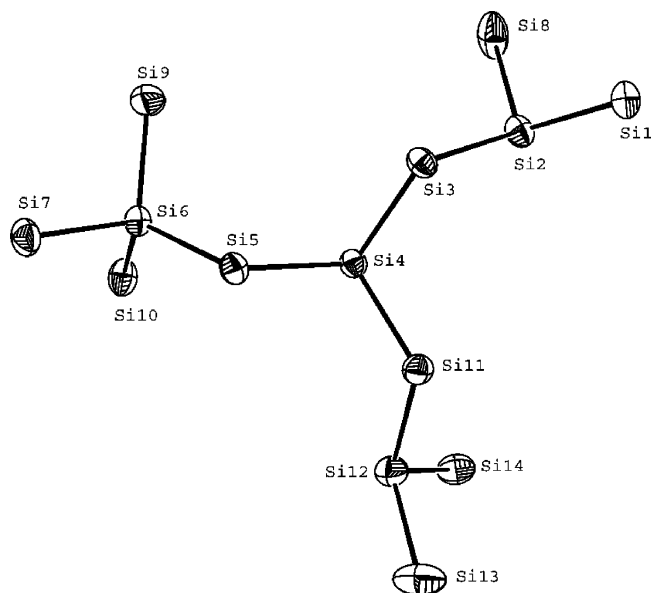


**Figure 2.** Molecular structure of **5** in the crystal state (ORTEP, 30% probability level, all methyl groups omitted for clarity). Selected bond lengths (Å), bond angles (deg), and dihedral angles (deg): Si3–Si4 = 2.384(1), Si5–Si6 = 2.379(1), Si5–Si4 = 2.392(1), Si11–Si4 = 2.387(1); Si2–Si3–Si4 = 115.83(5), Si6–Si5–Si4 = 119.30(5), Si12–Si11–Si4 = 115.53(5); Si14–Si12–Si11–Si4 = 84.21(7), Si4–Si5–Si6–Si9 = 61.70(8), Si4–Si5–Si6–Si10 = 62.40(7), Si2–Si3–Si4–Si11 = 81.94(7), Si2–Si3–Si4–Si5 = 162.30(5), Si12–Si11–Si4–Si3 = 159.63(5), Si6–Si5–Si4–Si3 = 98.47(6), Si4–Si3–Si2–Si1 = 137.98(6), Si4–Si3–Si2–Si8 = 103.16(7), Si4–Si5–Si6–Si7 = 179.81(5), Si6–Si5–Si4–Si11 = 146.80(5), Si12–Si11–Si4–Si5 = 81.84(7), Si13–Si12–Si11–Si4 = 155.98(6).

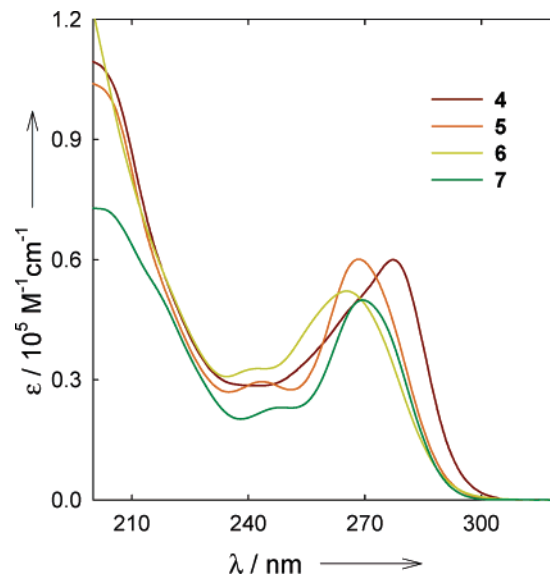


**Figure 3.** UV spectra of **4–7** in solution.

calculated average Si–Si distances of each of the heptasilane chains lie unremarkably within the relatively narrow range of 2.36–2.39 Å, which suggests only minimal, if not negligible, influence of Si–Si bond stretching on the energy of the  $\sigma$  to  $\sigma^*$  transition in these compounds.<sup>13</sup>

The UV absorption spectra of **4–7** at 293 K are shown in Figures 3 and 4, and the data are summarized in Table 2 together

(13) Casher, D. L.; Tsuji, H.; Sano, A.; Katkevics, M.; Toshimitsu, A.; Tamao, K.; Kubota, M.; Kobayashi, T.; Ottosson, C. H.; David, D. E.; Michl, J. *J. Phys. Chem. A* **2003**, 107, 3559.



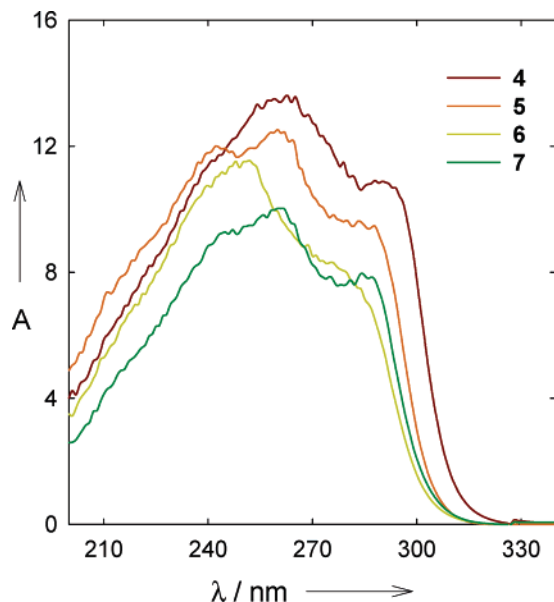


Figure 4. UV spectra of 4–7 in the solid state (diffuse reflectance).

Table 2. UV Spectroscopic Properties of Single-Core Dendrimers 4–8

compd	solution			solid state	
	$\lambda_{\max}$ (nm)	$10^{-4}\epsilon$	band gap (nm)	$\lambda_{\max}$ (nm)	band gap (nm)
4	277	6.0	294	291	310
5	269	6.0	290	284	304
6	265	5.2	290	280	303
7	269	5.0	291	285	304
8 <sup>15</sup> (293 K)	269	2.9			
8 <sup>15</sup> (77 K)	274	9.5			

with those of the linear heptasilane *n*-Si<sub>7</sub>Me<sub>16</sub> (**8**). In solution (heptane,  $c = 10^{-5}$  M), the unconstrained dendrimers **5**, **7**, and **8** exhibit absorption maxima at 269 nm with band gaps of around 290–291 nm. Owing to the presence of a variety of different conformers that are contributing differently to the energy of the  $\sigma$  to  $\sigma^*$  transition, dendrimer **6** exhibits a much broader UV curve with a somewhat blue-shifted absorption maximum at 265 nm<sup>14</sup> and a band gap of around 290 nm, which is identical with those of **5** and **7**. In striking contrast, the UV absorption curve of tethered **4** shows a considerably red-shifted absorption maximum at 277 nm, which is accompanied by a shoulder at around 268 nm. The absorption maximum of **4** is also shifted to longer wavelength relative to that of *n*-Si<sub>7</sub>Me<sub>16</sub> (**8**)<sup>15</sup> at 77 K, where the chain most likely adopts an all-anti conformation that is optimal for  $\sigma$ -conjugation. Assuming the conformational arrangement of **4** in the solid state to be similar to that in solution, it can be concluded that the absorption maximum of **4** corresponds to a conformer with large dihedral angles such as A–D–A–D, whereas the shoulder at 268 nm may arise from the A–D–O–A and D–G–O–A conformers, similar to those observed for the unconstrained dendrimers.

Interestingly, the same trends mentioned before are seen in the solid-state spectra, although the band gaps and absorption maxima of **4**–**7** are red-shifted by ca. 15 nm. This can be understood in terms of intermolecular electronic interactions in the solid state, which lower the optical band gap in solids. However, the absorption maximum of tethered **4** (ca. 291 nm) is red-shifted

ca. 7–8 nm relative to those of **5** and **7**. The good agreement of the optical trends in solution and the solid-state spectra is extremely useful, as one can correlate the solid-state conformation of the oligosilane chains obtained from X-ray data with the optical properties of these highly flexible molecules in solution. In this context, diffuse-reflectance UV spectroscopy can provide useful insights into the relationship between silicon backbone conformation and electronic properties of these materials.

In conclusion, our findings for dendritic oligosilanes are in full agreement with those of Michl<sup>3a</sup> and Tamao,<sup>3b–d</sup> who elegantly demonstrated by incorporation of linear tetrasilane and hexasilane moieties into rigid cyclic carbosilane compounds that the absorption maximum arises mainly from the all-anti conformers in the oligosilane chains and that additional ortho or gauche fragments do not significantly contribute to the elongation of  $\sigma$ -conjugation. We have shown that single-core oligosilane dendrimers, unless they are incorporated into a carbocyclic ring system as in tethered **4**, cannot maintain an all-anti-conformation in the longest heptasilane chains.

## Experimental Section

**General Procedure.** All manipulations of air- and/or moisture-sensitive compounds were carried out under an atmosphere of argon using standard Schlenk and glovebox techniques. THF, *n*-heptane, and *n*-pentane were distilled under argon from alkali metals prior to use. The compounds MeSi(SiMe<sub>3</sub>)<sub>16</sub> and MeSi(SiMe<sub>2</sub>Cl)<sub>17</sub> were synthesized according to literature procedures. The potassium silanides KSi(SiMe<sub>3</sub>)<sub>2</sub>Me and KSi(SiMe<sub>3</sub>)<sub>3</sub> have been prepared according to a procedure described by Marschner.<sup>18</sup> The compounds (SiMe<sub>3</sub>)<sub>3</sub>Si(CH<sub>2</sub>)<sub>4</sub>Si(SiMe<sub>3</sub>)<sub>3</sub> (**2**) and K(SiMe<sub>3</sub>)<sub>2</sub>Si(CH<sub>2</sub>)<sub>4</sub>Si(SiMe<sub>3</sub>)<sub>2</sub>K (**3**) were synthesized by a modified literature procedure.<sup>8</sup> Microanalyses were carried out with a Thermoquest Flash EA 1112 C/H/N/S-Analyzer by addition of Pb<sub>3</sub>O<sub>4</sub> for silicon-containing compounds. NMR: Bruker AC 250 and Bruker ARX 300. UV/vis: Perkin-Elmer Lambda 2, quartz cells of 1.0 cm path length and spectral grade *n*-heptane. The diffuse-reflectance UV measurements were carried out with a Perkin-Elmer Lambda 20 instrument.

**1-Chloro-2-(chlorodimethylsilyl)-1,1,2,3,3,5,5,5-octamethyl-4,4-bis(trimethylsilyl)pentasilane (1).** In a Schlenk flask with a magnetic stirrer were rapidly placed Si(SiMe<sub>3</sub>)<sub>4</sub> (5 g, 15.58 mmol) and Bu<sup>t</sup>OK (1.75 g, 15.58 mmol). The flask was evacuated and refilled with argon three times, THF (40 mL) was added, and the yellow solution of KSi(SiMe<sub>3</sub>)<sub>3</sub>, which formed within several hours, was stirred overnight. After the solvent was changed to *n*-pentane, the resulting solution was slowly added to a vigorously stirred *n*-pentane solution of (ClMe<sub>2</sub>Si)<sub>3</sub>SiMe (4.04 g, 12.46 mmol) at –78 °C. After it was stirred for 30 min at –78 °C, the mixture was warmed to room temperature within 2 h. The resulting suspension was filtered, and the filtrate was evaporated under vacuum. Distillation of the residue under vacuum in a Kugelrohr furnace (160–170 °C, 0.01 mbar) afforded 4.61 g (69%) of the title compound as a solid. Mp: 98–100 °C. <sup>1</sup>H NMR (C<sub>6</sub>D<sub>6</sub>, 250 MHz):  $\delta$  0.59 (s, SiMe<sub>2</sub>, 6 H), 0.58 (s, SiMe<sub>2</sub>Cl, 12 H), 0.31 (s, SiMe, 3 H), 0.30 (s, SiMe<sub>3</sub>, 27 H) ppm. <sup>13</sup>C NMR (C<sub>6</sub>D<sub>6</sub>, 75.5 MHz):  $\delta$  5.7 (SiMe<sub>2</sub>Cl), 3.6 (SiMe<sub>3</sub>), 3.1 (SiMe<sub>2</sub>), –9.0 (SiMe) ppm. <sup>29</sup>Si NMR (C<sub>6</sub>D<sub>6</sub>, 59.6 MHz):  $\delta$  29.4 (SiMe<sub>2</sub>Cl), –9.4 (SiMe<sub>3</sub>), –29.7 (SiMe<sub>2</sub>), –72.3 (SiMe), –125.9 (SiSi<sub>4</sub>) ppm. Anal. Calcd for C<sub>16</sub>H<sub>48</sub>Cl<sub>2</sub>Si<sub>8</sub> (536.142): C, 35.84; H, 9.02; Cl, 13.23. Found: C, 35.61; H, 8.78; Cl, 13.01.

**1,1,1,8,8,8-Hexamethyl-2,2,7,7-tetrakis(trimethylsilyl)-1,2,7,8-tetrasilaoctane (2).** 1,4-Dibromobutane (3.3 g, 15.28 mmol)

(16) Marsmann, H. C.; Raml, W.; Hengge, E. *Z. Naturforsch., B* **1980**, *35B*, 1541.

(17) Herzog, U.; Schulze, N.; Trommer, K.; Roewer, G. *J. Organomet. Chem.* **1997**, *547*, 133.

(18) Marschner, C. *Eur. J. Inorg. Chem.* **1998**, 221.

(14) The observed values for the absorption maximum of dendrimer **6** reported herein are in contrast with those observed by Lambert<sup>9a,b</sup> ( $\lambda_{\max}$  272 nm;  $\epsilon = 3.4 \times 10^5$ ; 298 K, hexane).

(15) Obata, K.; Kira, M. *Organometallics* **1999**, *18*, 2216.

dissolved in *n*-pentane (50 mL) was slowly added to a vigorously stirred *n*-pentane solution of  $\text{KSi}(\text{SiMe}_3)_3$  (derived from  $\text{Si}(\text{SiMe}_3)_4$  (10 g, 31.17 mmol) and  $\text{Bu}^t\text{OK}$  (3.495 g, 31.17 mmol) in THF) at  $-78^\circ\text{C}$ . After it was stirred for 2 h at  $-78^\circ\text{C}$ , the reaction mixture was warmed to room temperature. Water was added with stirring to the resulting suspension, the organic layer was separated, and the aqueous layer was extracted twice with pentane. The combined organic extracts were dried over  $\text{MgSO}_4$  and filtered, and the solvent was evaporated under vacuum. The residue was suspended in ethanol, filtered, and dried under vacuum to give crude **2** contaminated by  $\text{Si}(\text{SiMe}_3)_4$ . After sublimation of  $\text{Si}(\text{SiMe}_3)_4$  (0.01 mbar,  $120^\circ\text{C}$ ) from the mixture, crude **2** was recrystallized from acetone. Yield 5.98 g (71%). Mp:  $136^\circ\text{C}$ .  $^1\text{H}$  NMR ( $\text{CDCl}_3$ , 250 MHz):  $\delta$  1.41–1.35 (m,  $\text{CH}_2\text{CH}_2$ , 4 H), 0.77–0.70 (m,  $\text{SiCH}_2$ , 4 H), 0.16 (s,  $\text{SiMe}_3$ , 54 H) ppm.  $^{13}\text{C}$  NMR ( $\text{CDCl}_3$ , 75.5 MHz):  $\delta$  34.0 ( $\text{CH}_2\text{-CH}_2$ ), 7.1 ( $\text{SiCH}_2$ ), 1.2 ( $\text{SiMe}_3$ ) ppm.  $^{29}\text{Si}$  NMR ( $\text{CDCl}_3$ , 59.6 MHz):  $\delta$   $-12.9$  ( $\text{SiMe}_3$ ),  $-81.9$  (Si) ppm. Anal. Calcd for  $\text{C}_{22}\text{H}_{62}\text{-Si}_8$  (551.412): C, 47.92; H, 11.33. Found: C, 47.82; H, 11.29.

**2,2,3,4,4-Pentamethyl-1,1,5,5-tetrakis(trimethylsilyl)-3-[2',2'-bis(trimethylsilyl)-1',1',1',3',3'-pentamethyltrisilanyl]-1,2,3,4,5-pentasilacyclononane (4)**. A solution of **1** (0.55 g, 1.03 mmol) in *n*-pentane (10 mL) was slowly added at  $-78^\circ\text{C}$  to a vigorously stirred THF solution of  $\text{K}(\text{Me}_3\text{Si})_2\text{Si}(\text{CH}_2)_4\text{Si}(\text{SiMe}_3)_2\text{K}$  (derived from **2** (0.6 g, 1.09 mmol) and  $\text{Bu}^t\text{OK}$  (0.244 mg, 2.18 mmol) in THF at  $65^\circ\text{C}$ ). After it was stirred for 2 h at  $-78^\circ\text{C}$ , the reaction mixture was warmed to room temperature. After water was added to the stirred suspension, the organic layer was separated and the aqueous layer was extracted twice with pentane. The combined organic extracts were dried over  $\text{MgSO}_4$ , filtered, concentrated, and kept under vacuum ( $10^{-2}$  mbar,  $150^\circ\text{C}$ ) for several hours to remove volatile byproducts. Purification of the crude product by column chromatography on silica gel (*n*-heptane) and subsequent recrystallization from ethyl acetate afforded the title compound as a white solid. Yield 0.25 g (28%). Mp:  $105^\circ\text{C}$ .  $^1\text{H}$  NMR ( $\text{C}_6\text{D}_6$ , 250 MHz):  $\delta$  1.74, 1.03 (2 m,  $\text{CH}_2$ ,  $2 \times 4$  H), 0.74 (s,  $\text{SiMe}$ , 3 H), 0.69, 0.65, 0.63 (3 s,  $\text{SiMe}_2$ ,  $3 \times 12$  H), 0.38 (s,  $\text{Si}(\text{SiMe}_3)_3$ , 27 H), 0.32, 0.30 (2 s,  $\text{Si}(\text{SiMe}_3)_2$ ,  $2 \times 18$  H).  $^{13}\text{C}$  NMR ( $\text{C}_6\text{D}_6$ , 75.5 MHz):  $\delta$  29.6, 6.1 ( $\text{CH}_2$ ), 3.1, 1.6, 0.9 ( $\text{SiMe}_2$ ), 2.3 ( $\text{Si}(\text{SiMe}_3)_3$ ), 0.1, 0.0 ( $\text{Si}(\text{SiMe}_3)_2$ ),  $-5.9$  ( $\text{SiMe}$ ) ppm.  $^{29}\text{Si}$  NMR ( $\text{C}_6\text{D}_6$ , 59.6 MHz):  $\delta$   $-9.2$ ,  $-10.9$ ,  $-12.8$  ( $\text{SiMe}_3$ ),  $-22.7$ ,  $-29.1$ ,  $-57.6$  ( $\text{SiMe}_2$ ),  $-70.2$ ,  $-94.8$  ( $\text{SiMe}$ ),  $-121.7$  ( $\text{SiSi}_4$ ). Anal. Calcd for  $\text{C}_{32}\text{H}_{92}\text{Si}_{14}$  (870.27): C, 44.16; H, 10.66. Found: C, 43.96; H, 10.62.

**1,1,1,2,3,3,4,5,5,6,7,7,7-Tridecamethyl-2,6-bis(trimethylsilyl)-4-[2',2'-bis(trimethylsilyl)-1',1',1',3',3'-pentamethyltrisilanyl]heptasilane (5)**. A solution of **1** (1 g, 1.87 mmol) in *n*-pentane (10 mL) was transferred via cannula to a vigorously stirred *n*-pentane solution of  $\text{KSi}(\text{SiMe}_3)_2\text{Me}$  (derived from  $\text{Si}(\text{SiMe}_3)_3\text{Me}$  (1.28 g, 4.87 mmol) and  $\text{Bu}^t\text{OK}$  (0.546 g, 4.87 mmol) in THF) at  $-78^\circ\text{C}$ . After it was stirred for 2 h at  $-78^\circ\text{C}$ , the reaction mixture was

warmed to room temperature. After water was added to the stirred suspension, the organic layer was separated and the aqueous layer was extracted twice with pentane. The combined organic extracts were dried over  $\text{MgSO}_4$  and filtered, and the solvent was evaporated. Recrystallization of the residue from acetone afforded 1.24 g (78%) of the title compound. Mp:  $144^\circ\text{C}$ .  $^1\text{H}$  NMR ( $\text{C}_6\text{D}_6$ , 250 MHz):  $\delta$  0.70 (s,  $\text{SiMe}$ , 3 H), 0.68 (s,  $\text{SiMe}$ , 6 H), 0.61, 0.60, 0.42 (3 s,  $\text{SiMe}_2$ ,  $3 \times 12$  H), 0.38 (s,  $\text{Si}(\text{SiMe}_3)_2$ , 36 H), 0.29 (s,  $\text{Si}(\text{SiMe}_3)_3$ , 27 H) ppm.  $^{13}\text{C}$  NMR ( $\text{C}_6\text{D}_6$ , 75.5 MHz):  $\delta$  4.7, 2.7, 2.7 ( $\text{SiMe}_2$ ), 4.2, 1.3 ( $\text{SiMe}_3$ ),  $-4.4$ ,  $-9.2$  ( $\text{SiMe}$ ) ppm.  $^{29}\text{Si}$  NMR ( $\text{C}_6\text{D}_6$ , 59.6 MHz):  $\delta$   $-9.2$ ,  $-11.1$  ( $\text{SiMe}_3$ ),  $-25.1$ ,  $-29.3$ ,  $-59.9$  ( $\text{SiMe}_3$ ),  $-79.2$  ( $\text{SiMe}$ ),  $-123.0$  ( $\text{SiSi}_4$ ) ppm. Anal. Calcd for  $\text{C}_{30}\text{H}_{90}\text{Si}_{14}$  (844.233): C, 42.68; H, 10.75. Found: C, 42.74; H, 10.96.

**Crystal Data for 4 (CCDC 620793)**. The crystal ( $0.30 \times 0.17 \times 0.04$ ) was fixed with a perfluoropolyether on a tip of a thin glass rod. Intensity data for this crystal were then collected at 173(2) K on a Bruker X8 APEX diffractometer with a CCD camera, Mo  $\text{K}\alpha$  radiation ( $\lambda = 0.71073 \text{ \AA}$ ), and graphite monochromator: formula  $\text{C}_{32}\text{H}_{92}\text{Si}_{14}$ ,  $M_r = 870.32$ , triclinic, space group  $P\bar{1}$ ,  $a = 15.8567(16) \text{ \AA}$ ,  $b = 19.181(2) \text{ \AA}$ ,  $c = 21.504(2) \text{ \AA}$ ,  $\alpha = 69.222(6)^\circ$ ,  $\beta = 77.258(5)^\circ$ ,  $\gamma = 74.019(5)^\circ$ ,  $V = 5823.6(11) \text{ \AA}^3$ ,  $Z = 4$ ,  $\rho_{\text{calcd}} = 0.993 \text{ g cm}^{-3}$ ,  $\mu = 0.327 \text{ mm}^{-1}$ , 107 378 measured reflections, 24 399 independent reflections ( $R_{\text{int}} = 0.1731$ ), 885 parameters,  $R1(F) = 0.0674$  for 10 239 reflections with  $I > 2\sigma(I)$  and  $wR2(F^2) = 0.1362$  for all data, residual electron density highest peak  $0.464 \text{ e \AA}^{-3}$  and deepest hole  $-0.337 \text{ e \AA}^{-3}$ .

**Crystal Data for 5 (CCDC 620794)**. The crystal<sup>19</sup> ( $0.79 \times 0.13 \times 0.07 \text{ mm}^3$ ) was fixed with a perfluoropolyether on a tip of a thin glass rod. Intensity data for this crystal were then collected at 173(2) K on a Bruker X8 APEX diffractometer with a CCD camera, Mo  $\text{K}\alpha$  radiation ( $\lambda = 0.71073 \text{ \AA}$ ), and graphite monochromator: formula  $\text{C}_{30}\text{H}_{90}\text{Si}_{14}$ ,  $M_r = 844.28$ , monoclinic, space group  $C2/c$ ,  $a = 31.4168(8) \text{ \AA}$ ,  $b = 9.4634(3) \text{ \AA}$ ,  $c = 39.6320(10) \text{ \AA}$ ,  $\alpha = \gamma = 90^\circ$ ,  $\beta = 105.7510(10)^\circ$ ,  $V = 11340.5(5) \text{ \AA}^3$ ,  $Z = 8$ ,  $\rho_{\text{calcd}} = 0.989 \text{ g cm}^{-3}$ ,  $\mu = 0.334 \text{ mm}^{-1}$ , 20 457 measured reflections, 4628 independent reflections ( $R_{\text{int}} = 0.0344$ ), 427 parameters,  $R1(F) = 0.0332$  for 3812 reflections with  $I > 2\sigma(I)$  and  $wR2(F^2) = 0.0457$  for all data, residual electron density highest peak  $0.431 \text{ e \AA}^{-3}$  and deepest hole  $-0.195 \text{ e \AA}^{-3}$ .

**Supporting Information Available:** CIF files giving crystallographic data for **4** and **5**. This material is available free of charge via the Internet at <http://pubs.acs.org>.

OM060964K

(19) The Wilson plot led to an upper  $\theta$  limit of less than  $20^\circ$ . However, thicker crystals did not give better results during the data collections, as the calculations demonstrated.